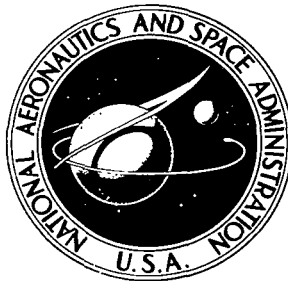


NASA TECHNICAL NOTE



NASA TN D-4783

c.1

NASA TN D-4783

LOAN COPY: RETI
AFWL (WLIL
KIRTLAND AFB, TX



MEASUREMENT OF THE
 $^{10}\text{B}(n,\alpha)^7\text{Li}$, $^7\text{Li}^*$ RELATIVE
CROSS SECTIONS IN THE keV REGION

by

Donald Bogart

Lewis Research Center

and

Lowell L. Nichols

Pacific Northwest Laboratory

NATIONAL AERONAUTICS AND SPACE ADMINISTRATION • WASHINGTON, D. C. • SEPTEMBER 1968





MEASUREMENT OF THE $^{10}\text{B}(n,\alpha)^7\text{Li}$, $^7\text{Li}^*$ RELATIVE CROSS SECTIONS
IN THE keV REGION

By Donald Bogart

Lewis Research Center
Cleveland, Ohio

and

Lowell L. Nichols

Pacific Northwest Laboratory
Richland, Wash.

NATIONAL AERONAUTICS AND SPACE ADMINISTRATION

For sale by the Clearinghouse for Federal Scientific and Technical Information
Springfield, Virginia 22151 - CFSTI price \$3.00

ABSTRACT

Relative cross sections for $^{10}\text{B}(n, \alpha)^7\text{Li}$, $^7\text{Li}^*$ were obtained from measurements of the counting ratios of a $^{10}\text{BF}_3$ proportional counter and a precision long counter used to monitor relative neutron fluxes. Monoenergetic neutrons were produced by a Van de Graaff accelerator in the energy region from 30 to 800 keV. When the relative cross sections are normalized to a $1/v$ variation below 80 keV, the data lie above a $1/v$ line from 80 to 550 keV indicating departures of 15 percent at 140 keV and 20 percent at 220 keV. Recommended cross sections for $^{10}\text{B}(n, \alpha)^7\text{Li}$, $^7\text{Li}^*$ up to 1 MeV are obtained from recently available measurements and the known levels in ^{11}B .

MEASUREMENT OF THE $^{10}\text{B}(n, \alpha)^7\text{Li}$, $^7\text{Li}^*$ RELATIVE CROSS SECTIONS IN THE keV REGION

by Donald Bogart and Lowell L. Nichols[†]

Lewis Research Center

SUMMARY

Relative cross sections for $^{10}\text{B}(n, \alpha)^7\text{Li}$, $^7\text{Li}^*$ were obtained from measurements of the counting ratios of a $^{10}\text{BF}_3$ proportional counter and a precision long counter used to monitor relative neutron fluxes. Monoenergetic neutrons were produced by a Van de Graaff accelerator in the energy region from 30 to 800 keV. When the relative cross sections are normalized to a $1/v$ variation below 80 keV, the data lie above a $1/v$ line from 80 to 550 keV indicating departures of 15 percent at 140 keV and 20 percent at 220 keV.

Measurements were also made of the relative efficiency of a modified long counter used by Bichsel and Bonner to monitor neutron flux in their measurements of the $^{10}\text{B}(n, \alpha)^7\text{Li}$, $^7\text{Li}^*$ cross sections. The Bichsel and Bonner cross sections also lie above a $1/v$ line from 80 to 220 keV when corrected for the efficiency of their flux monitor.

Recommended cross sections for $^{10}\text{B}(n, \alpha)^7\text{Li}$, $^7\text{Li}^*$ up to 1 MeV are obtained from recently available measurements and the known levels in ^{11}B .

INTRODUCTION

Because of the importance of the boron reaction as a neutron flux monitor in the measurement of capture cross sections in the keV region, $^{10}\text{B}(n, \alpha)$ cross sections have been measured by several methods recently. Mooring, Monahan, and Huddleston (ref. 1) measured the ratio of scattering to total cross sections and the total cross section to obtain the absorption cross section of ^{10}B . Cox and Pontet (ref. 2) reported an analysis of spherical shell transmission experiments to yield average values of the absorption cross section of ^{10}B . Macklin and Gibbons (ref. 3) arrived at values of the $^{10}\text{B}(n, \alpha)^7\text{Li}$, $^7\text{Li}^*$

[†]Pacific Northwest Laboratory, Richland, Washington.

cross section by reciprocity using measured ${}^7\text{Li}(\alpha, n){}^{10}\text{B}$ yields and $(n, \alpha_0)/(n, \alpha_1\gamma)$ branching ratios.

Nellis, et al. (refs. 4 and 5) have measured differential cross sections for the production of the 0.478-MeV gamma ray from ${}^{10}\text{B}$ and have obtained ${}^{10}\text{B}(n, \alpha_1\gamma)$ cross sections in the region from 300 to 1000 keV. Applying available branching ratios to these data provides values of the ${}^{10}\text{B}(n, \alpha)$ cross section. Davis, et al. (ref. 6) measured the ${}^{10}\text{B}(n, \alpha_0){}^7\text{Li}$ and ${}^{10}\text{B}(n, \alpha_1\gamma){}^7\text{Li}^*$ cross sections above 300 keV with a grid-type ionization chamber filled with ${}^{10}\text{BF}_3$ and argon using pulse-height spectra analysis.

Until the more recent measurements, the only boron absorption cross sections in the lower kilovolt region had been those of Bichsel and Bonner (ref. 7) who employed a ${}^{10}\text{BF}_3$ proportional counter and Van de Graaff produced neutrons from 20 keV to 4 MeV. Relative neutron fluxes had been monitored by a modified long counter using an efficiency that had been presumed to be constant with neutron energy. This modified long counter described by Bonner (ref. 8) had a much smaller surrounding paraffin thickness than the conventional long counter (ref. 9) and therefore would be expected to have an efficiency that varies considerably with neutron energy. Bogart (ref. 10) estimated an efficiency curve for this modified long counter that was necessary to remove discrepancies in several sets of reported capture cross sections for gold. The gold measurements had used the Bichsel and Bonner data for ${}^{10}\text{B}$ as a flux monitor. The use of this estimated efficiency curve to correct the Bichsel and Bonner data suggested a large departure from a $1/v$ variation in the ${}^{10}\text{B}$ absorption cross section above 80 keV with values indicated to be as much as 30 percent above $1/v$ at 150 keV.

Because of the development of the precision long counter for monitoring neutron fluxes (refs. 11 and 12) and to verify the accuracy of the widely used Bichsel and Bonner data, a program was undertaken using the Battelle-Northwest Van de Graaff accelerator. The program consisted of measuring ${}^{10}\text{B}(n, \alpha)$ counting rate as a function of neutron energy using a bare ${}^{10}\text{BF}_3$ counter similar to that used by Bichsel and Bonner. In addition, the efficiency of a reproduction of the modified long counter that had been used (ref. 7) was measured as a function of neutron energy. The precision long counter was employed as the flux monitor for all present measurements.

EXPERIMENT

The experiments were performed in the low-scattering room of the Battelle-Northwest positive-ion Van de Graaff accelerator. This room is 5.5 meters high, 8.5 meters wide, and 9.1 meters long and contains a centrally located pit 2.4 meters deep, 6.1 meters wide, and 6.4 meters long that is covered with a lightweight aluminum grating floor. All measurements were performed 1.1 meters above this grating floor in

a horizontal plane that contains the neutron-producing target that was located over the center of the pit. The beam duct extends 4.3 meters to the center of the room through a 50-centimeter-thick paraffin shield wall. The beam-bending magnets were located behind the paraffin shield wall, and the room was free of other concentrations of scattering materials. The nearest scattering wall is therefore the concrete floor of the pit which is 3.5 meters from the target.

Monoenergetic neutrons were obtained from charged-particle reactions. The following neutron-producing targets were employed: (1) lithium fluoride on tantalum backing for $\text{Li}(p, n)$ reactions (target thickness, $30 \mu\text{g}/\text{cm}^2$); (2) tritium loaded titanium on tantalum backing for $\text{T}(p, n)$ reactions (target thickness, $500 \mu\text{g}/\text{cm}^2$); and (3) titanium deuteride layers on tantalum backing for $\text{D}(d, n)$ reactions (target thickness, $310 \mu\text{g}/\text{cm}^2$). All tantalum backing thicknesses were 20 mils (0.508 mm) and the charged-particle beam was collimated to 1 centimeter in diameter. The targets were supported by a thin-walled stainless-steel holder and cooled by an air jet from a thin aluminum tube.

The accelerator positive-ion energy was calibrated using the $\text{Li}(p, n)$ threshold reaction at 1.8812 MeV. Energy control of the accelerator was monitored using a nuclear magnetic resonance gaussmeter.

Figure 1 shows the arrangement of the detectors relative to the neutron-producing

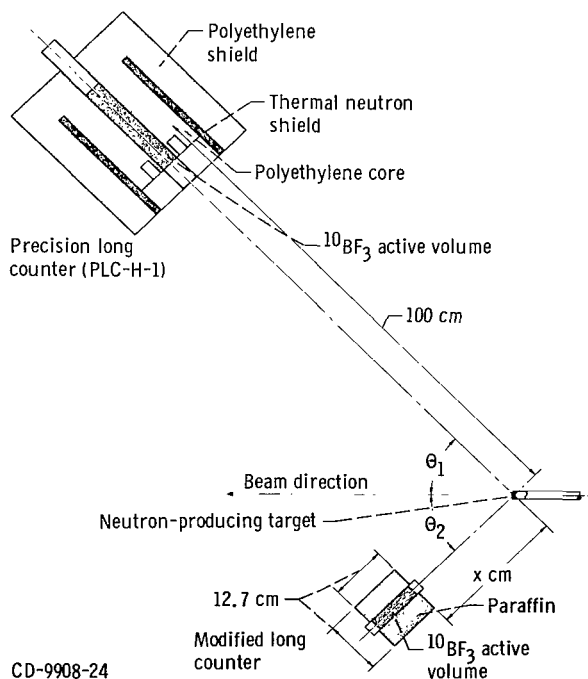


Figure 1. - Arrangement for calibrating modified long counter and bare $^{10}\text{BF}_3$ counter against precision long counter.

target. The precision long counter (PLC-H-1) and either the modified long counter or a bare $^{10}\text{BF}_3$ counter was positioned at symmetrical angles $\theta_1 = \theta_2$ relative to the direction of the ion beam. The modified long counter or bare $^{10}\text{BF}_3$ counter was supported by a lightweight aluminum table with the axis of the counter located along a radial line from the target. All positioning angles were determined by an instrument carrier. The radial positions of the front faces of the modified long counter and the bare $^{10}\text{BF}_3$ counter were located to ± 0.1 centimeter at each of four positions (values of x in fig. 1). The precision long counter was positioned by the instrument carrier at a constant distance $(x + c)$ of 100 centimeters, where x is the distance from the source to the front face of the $^{10}\text{BF}_3$ tube housing and c is the distance from the front face to the effective center of detection.

A discussion of the use of the long counter as an effective point detector is given by Allen (ref. 13). Since the long counter is used as a flux monitor and is a large mass of paraffin or polyethylene, with a central $^{10}\text{BF}_3$ counter, it is necessary to establish at what point the counter can be considered to be effectively concentrated. For a fixed calibration flux, DePangher (ref. 11) analyzed the counts A for various distances x of the precision long counter from the source by applying the following equation:

$$A = a + \frac{b}{(x + c)^2} \quad (1)$$

where a , b , and c are constants. This equation treats the count rate of a finite detector as equivalent to that of a point detector located $x + c$ centimeters from the point source. It presumes that the neutron flux incident on the counter face has the same energy and angular variation as the calibration flux and that room-scattered neutrons contribute a constant count a for all values of x over which the detector is employed. Thus, for the precision long counter, PLC-H-1 used herein, DePangher and Nichols (ref. 12) found for the same scattering room used in the present experiments, that

$$\frac{a}{b} = 2.5 \times 10^{-6}$$

$$c = 7.8 + 1.1 E$$

where E is energy in MeV, so that, at $x + c = 100$ centimeters, equation (1) for a unit room-scattered count rate provides

$$A = 1 + \frac{4 \times 10^5}{10^4} = 1 + 40$$

and room-scattered neutrons contribute about 2 percent to the count rate of PLC-H-1. As a check, a second precision long counter (PLC-H-2) was used as a monitor in preliminary measurements, while the background response of PLC-H-1 was measured at all target angles and for several neutron energies. It was corroborated that backgrounds in PLC-H-1 were less than 2 percent for all cases. Subsequent measurements did not involve this secondary monitor which was removed.

For the case of $^{10}\text{BF}_3$ counters in paraffin moderators smaller than those used in the precision long counter and including a paraffin thickness used in the modified long counter, DePangher (ref. 14) demonstrated the utility of equation (1) to separate direct count rate from that of room-scattered neutrons.

In the analysis of the present experiments, equation (1) has been applied to the bare $^{10}\text{BF}_3$ counter data to separate counts due to "monoenergetic" incident neutrons from counts due to room-scattered neutrons. Because of the finite solid angle subtended by the active volume of the $^{10}\text{BF}_3$ counter and the anisotropy in yield and energy for the neutron-producing target reactions, the data are not monoenergetic. The energy resolution of the counter events due to the energy variation of incident source neutrons and counter wall scatterings has been calculated and is discussed later. It is shown that, although the $^{10}\text{BF}_3$ and argon gases in the counter are relatively transparent to incident neutrons, the brass walls of the counter are relatively thick so that wall scatterings are important in distributing the counter events more uniformly within the active volume.

BARE $^{10}\text{BF}_3$ COUNTER

For detection of $^{10}\text{B}(n, \alpha)^7\text{Li}$, $^7\text{Li}^*$ events, a brass BF_3 neutron counter was used that was filled with gas enriched to 96 percent in ^{10}B at a pressure of 45 centimeters of mercury ($59\,850\text{ N/m}^2$) and containing additional argon at a partial pressure of 90 centimeters of mercury ($119\,700\text{ N/m}^2$). The $^{10}\text{BF}_3$ counter is shown schematically in figure 2. The counter is 2.54 centimeters in outside diameter with brass walls 0.089 centimeter thick. The active volume is positioned symmetrically in a 15.4-centimeter length of tube and is 11.4 centimeters long.

Measurements of the pulse-height distributions for this $^{10}\text{BF}_3$ tube clearly showed the good resolution of the main peak produced from the $^{10}\text{B}(n, \alpha_1\gamma)^7\text{Li}^*$ reaction. The smaller peak produced from the ground-state reaction $^{10}\text{B}(n, \alpha_0)^7\text{Li}$ was also clearly seen. The method for setting the gain and the bias of the counting system to ensure reproducibility has been described in detail in references 11 and 12. Briefly, the method for adjusting the gain exploits the good resolution of the $^{10}\text{BF}_3$ tube and compares integral counting rates at two discriminator levels: one a low level chosen at an insensitive flat region of the pulse-height distribution and the other a higher level chosen

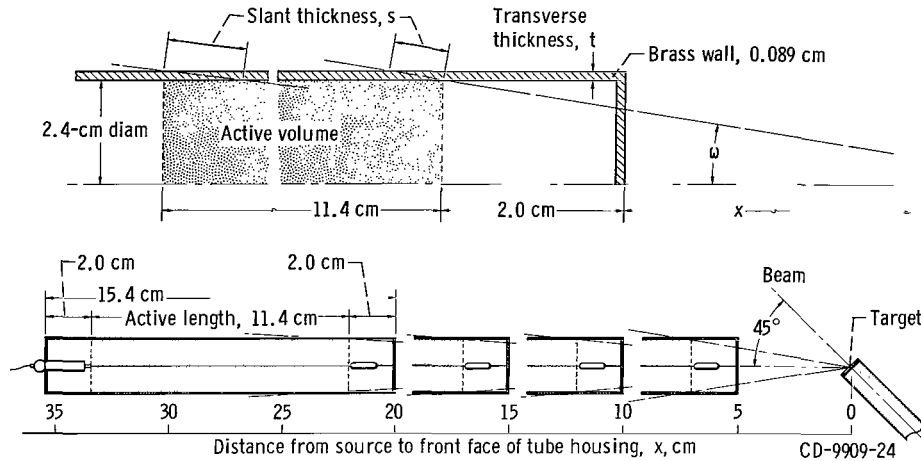


Figure 2. - Radial positions and geometry of brass $^{10}\text{BF}_3$ counter in neutron field.

at a sensitive rapidly varying part of the main peak of the distribution. If the gain were set correctly, the integral counting rates at the two discriminator levels would have a fixed ratio. This fixed ratio provided a criterion for maintaining accurately reproducible values of low bias integral counting rates. A voltage plateau and a differential pulse-height spectrum were taken twice for each counter: once at the beginning of the measurements and again at the conclusion of the work. There was no observable change in either the plateau or pulse-height spectrum over this period.

Counts were measured at several radial positions from the target for each neutron energy using the PLC-H-1 as a neutron flux monitor (see fig. 1). Radial distances to the front face of the brass counter were 5, 10, 15, and 20 centimeters, respectively. The radial positions and geometry of the BF_3 counter at 45° to the beam direction are illustrated in figure 2, and the overlapping positions of the active volumes are noted. The gas in the counter is about 1 percent of a total mean free path in thickness and is therefore transparent to incident neutrons in the keV region. The brass walls of the counter are about 5 percent of a total mean free path in transverse thickness t so that the front face of the counter is also relatively transparent to incident neutrons. However, the neutrons colliding with the cylindrical walls of the counter see a much thicker slant thickness s given by

$$s = \frac{t}{\sin \omega}$$

where ω is angle with counter axis.

Of those incident neutrons traversing the active volume, fractions from 25 percent at x of 7 centimeters to 75 percent at x of 33 centimeters collide with the side walls; about half of these are isotropically scattered back into the active volume. Scattering

collisions with the brass walls slightly alter the energy of the incident neutrons but significantly alter the volume distribution of events in the active volume.

The counts due to wall-scattered neutrons are calculated to be almost uniform along the active volume and to comprise about 20 percent of the direct counts. These calculations have been made numerically by dividing the frontal area of the active volume into 52 unit areas and employing line-of-sight average track length, average neutron energy, average source differential yield, and an average reaction cross section for each unit area and the solid angle it subtends from the source.

The results of the calculations for the relative counts of source neutrons and those neutrons that are scattered by the counter walls and reenter the active volume are shown in figure 3. The distribution of events is for the $^{10}\text{BF}_3$ counter in its closest position to the source at a distance x of 5 centimeters and for a $\text{Li}(p, n)$ target at 45° producing neutrons of nominal energy of 124 keV. The calculated distribution shows events to have occurred from 101 to 147 keV although 90 percent of all events occur within 124 ± 15 keV. The energy resolution has been chosen to be the width at half maximum; the energy resolution for the detector including the kinematic effects of the source is then 22 keV at a neutron energy of 124 keV. Energy resolutions have been determined in the same way for the other neutron energies.

The neutron-producing targets used were all relatively thin. Most of the data points

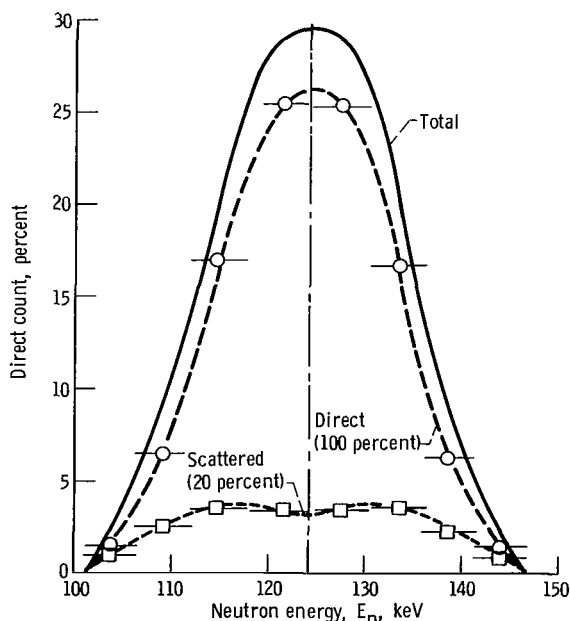


Figure 3. - Calculated distribution of direct and wall-scattered counts for $^{10}\text{BF}_3$ counter at $x = 5$ centimeters and for neutrons of nominal energy of 124 keV.

were taken using the Li(p, n) source reaction for which the proton energy loss in the target was very closely 3.8 keV for all proton energies. The spread in nominal neutron energy for these points varied from 3 percent at the lower energies to 1 percent at 200 keV. Therefore, the effects of the finite thickness of the target are small.

Because of the significant contribution of wall-scattered events, the concept of an effective center of detection for the bare $^{10}\text{BF}_3$ counter, as represented by equation (1), may be applied to the measured counts A:

$$A = a + \frac{b}{(x + c)^2} \quad (1)$$

where

a room-scattered background counts

b direct counts when center of detection is 1 cm from source

c distance of effective center of detection from front face

The value of b for the BF_3 counter is proportional to the product of the neutron flux φ and $^{10}\text{B}(n, \alpha)$ cross section σ :

$$b_{\text{BF}_3} \propto \varphi_{\text{BF}_3} \sigma(n, \alpha)$$

The value of b for the PLC-H-1 flux monitor is proportional to its calibrated efficiency η_{PLC} :

$$b_{\text{PLC}} \propto \varphi_{\text{BF}_3} \eta_{\text{PLC}}$$

or

$$^{10}\text{B}_{\sigma(n, \alpha)} \propto \frac{b_{\text{BF}_3}}{b_{\text{PLC}}} \eta_{\text{PLC}}$$

Values of η_{PLC} were obtained from experiments performed (ref. 12) with accelerator-produced neutrons at 45° and 75° in the same scattering room employed for the present experiments. The variation of η_{PLC} over the entire range of neutron energies studied is small increasing gradually from 0.95 at 30 keV to 1.00 at 500 keV. In the present experiments the precision long counter (PLC-H-1) was located at a constant distance $x + c$ of 100 centimeters from the source with the value of x adjusted with neutron energy to maintain $x + c$ constant (ref. 12).

The counts of the bare $^{10}\text{BF}_3$ counter were recorded for a fixed number of counts of PLC-H-1 (500 000 counts). The relative direct counts have been converted to boron cross sections by normalizing the results below 80 keV to a $1/v$ variation using an $^{10}\text{B}(n, \alpha)$ cross section of 3840 barns at 0.0253 eV.

MODIFIED LONG COUNTER

For detection of the $^{10}\text{B}(n, \alpha)^7\text{Li}$, $^7\text{Li}^*$ reaction, Bichsel and Bonner (ref. 7) used a brass $^{10}\text{BF}_3$ counter essentially identical to the one used in the present experiments. In their experiments, the front of the counter was located 3 centimeters from neutron-producing targets, and the sides of the counter were coated with approximately 0.5 millimeter of ^{10}B to reduce background due to room-scattered thermal neutrons. The background effect was obtained by moving the counter from its position close to the target to a position 85 centimeters from the target. It was stated that the largest background from room neutrons were observed at a neutron energy of 2 MeV and was measured to be less than 10 percent.

In the important energy range from 20 to 240 keV, neutrons were obtained from the $^7\text{Li}(p, n)$ reaction at 120° . The approximate detector geometry that had been used by Bichsel and Bonner is shown in figure 4. Relative neutron fluxes were monitored by a

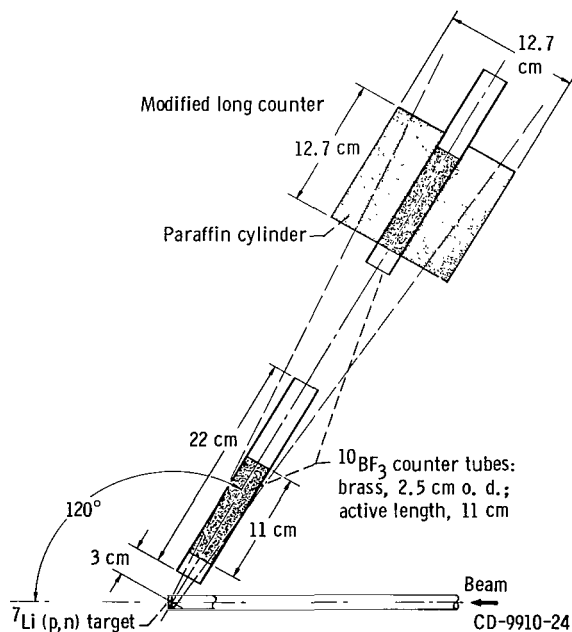


Figure 4. - Approximate detector geometry used by Bichsel and Bonner (ref. 6) for $^{10}\text{B}(n, \alpha)$ measurements for neutrons from 20 to 240 keV.

modified long counter presumably located behind the $^{10}\text{BF}_3$ counter. The close coupling was made possible by the reduced frontal area of the modified long counter. The efficiency of this counter had been presumed to be flat with energy. For a description of the counter used, Bichsel referred to Bonner, et al. (ref. 8) from which the following is quoted:

The neutron detector used was a modified long counter with a paraffin moderator 12.7 cm in diameter and 12.7 cm long surrounding a BF_3 counter which was 2.54 cm in diameter and extended to the front face of the paraffin. This smaller and more compact counter was used in place of a long counter so that considerable angular resolution could be obtained with the counter in a position such that its paraffin face was only 12.7 cm from the target. Under such geometrical conditions, the background counts were small in comparison to the counts from thin targets of the elements that were investigated. The modified long counter does not have an exactly flat response, independent of neutron energy; its efficiency for counting 4-MeV neutrons is only 60 percent as great as for 1-MeV neutrons.

The modified long counter deviates considerably from a conventional long counter of Hanson and McKibben (ref. 9) in both size and relative energy response. If a calibration of the efficiency of this counter were available, the reported boron cross sections of Bichsel and Bonner could be corrected for the flat response function that had been assumed. However, a further source of concern is the close coupling of the BF_3 counter and the modified long counter (fig. 4) and the mutual neutron scattering that can occur. The interactions of the brass walls of the BF_3 counter and the paraffin of the modified long counter introduce scattering effects that may be neutron-energy dependent. Furthermore, in reference 7, neutrons from 80 to 600 keV were obtained from the $^7\text{Li}(p, n)$ reaction at 0° . These experiments in the forward direction require a collinear setup of BF_3 counter and modified long counter flux monitor if simultaneous count rates are taken. Over this range of neutron energies, significant scattering perturbations to the BF_3 count rate and to the relative fluxes monitored by the modified counter may have been introduced. Therefore, the relative cross sections for $^{10}\text{B}(n, \alpha)^7\text{Li}$, $^7\text{Li}^*$ as reported by Bichsel and Bonner, even if corrected for the variation of efficiency of the modified counter, may still be in error because of the energy-dependent mutual scattering effects of the brass $^{10}\text{BF}_3$ detector directly in front of the modified long counter in their experiments.

In the present experiments, a reproduction of the modified long counter was constructed using an essentially identical $^{10}\text{BF}_3$ tube and surrounding paraffin cylinder. The count rate of the counter was measured at each of four radial positions from the target for each neutron energy using the symmetrically placed PLC-H-1 as a neutron flux

monitor (see fig. 1). Radial distances to the front face of the paraffin cylinder were 20, 30, 40, and 50 centimeters, respectively. Count rates of the counter were recorded for a fixed count of PLC-H-1 (600 000 counts). The direct count rate as a function of neutron energy was obtained by applying equation (1) to the data.

As previously described for the bare $^{10}\text{BF}_3$ counter, measurements of the relative efficiency for the modified long counter are given by:

$$\eta_{\text{MLC}} \propto \frac{b_{\text{MLC}}}{b_{\text{PLC}}} \eta_{\text{PLC}}$$

RESULTS

Table I lists our results for the bare BF_3 counter for neutron energies from 30 to 800 keV and the source reaction used. Values of the parameters b and c of equation (1) have been obtained by graphical analyses. With the known efficiency of the precision long counter and normalization to a $1/v$ variation below 80 keV, the listed values of $^{10}\text{B}_{\sigma(n, \alpha)}$ are obtained. Table II lists our results for the modified long counter for neutron energies from 40 to 3900 keV and the source reaction used. The parameters are again obtained by graphical analyses. Values of relative efficiency η_{MLC} , normalized at 120 keV, are listed.

Figures 5 and 6 illustrate representative analyses for the bare $^{10}\text{BF}_3$ counter and the modified long counter for a nominal neutron energy of 124 keV. A plot of $A(x + c)^2$ against $(x + c)^2$ should be linear for a reasonable value of c , the distance of the front face of the counter to its effective center of detection. There are best values of c that result in straight lines for both the bare BF_3 counter and the modified long counter. The slopes of the straight lines correspond to the background counts. The intercepts on the ordinates are the values of b with uncertainties corresponding to those in the best value of c . The uncertainties in b are obtained by examination of the curvature of the lines in figures 5 and 6 for a large range of c . The data shown in figure 5 indicate a change in curvature to occur between values of 6.5 and 7.0 centimeters and suggest a best value for c of 6.8 ± 0.2 centimeters.

For the bare BF_3 counter data shown in figure 5, 25 000 counts were measured at an x of 5 centimeters with the direct count rate about twice the background count rate. For the modified counter data shown in figure 6, 4 200 000 counts were measured at an x of 20 centimeters with the direct count rate 100 times the background count rate. In order to check the approximate spectral distribution of the background counts, data at 105 keV and at 153 keV were taken with a bare $^{10}\text{BF}_3$ tube and with the same $^{10}\text{BF}_3$ tube with

TABLE I. - RELATIVE CROSS SECTIONS FOR $^{10}\text{B}(n, \alpha)^7\text{Li}$, $^7\text{Li}^*$ FROM BARE $^{10}\text{BF}_3$ COUNTER AND PRECISION LONG COUNTER FLUX MONITOR

Neutron energy, E_n , keV	Source reaction	Counter angle, deg	Effective center of detection, c, cm	Relative $^{10}\text{BF}_3$ count	Efficiency of flux monitor, η_{PLC}	Cross section, $^{10}\text{B}\sigma(n\alpha)$, b ^a	
29±6	Li(p, n)	75	6.3±0.2	44.0±1.5	0.952	3.79±0.13	
39±7			6.7±0.2	35.3±0.9	.953	3.05±0.08	
44±7			6.5±0.2	34.4±1.0	.954	2.96±0.09	
58±8			6.7±0.2	29.8±0.7	.955	2.58±0.07	
58±8			6.4±0.2	28.1±0.9	.955	2.43±0.08	
67±8			6.4±0.2	27.3±0.8	.956	2.36±0.07	
76±9			6.5±0.2	25.8±0.7	.957	2.23±0.06	
80±9			6.6±0.2	25.6±0.7	.958	2.21±0.06	
105±10			45	6.7±0.2	23.5±0.6	.961	2.04±0.05
105±10			45	6.6±0.2	22.5±0.6	.961	1.95±0.05
120±11			60	6.6±0.2	21.6±0.6	.962	1.88±0.05
124±11			45	6.6±0.2	23.4±0.6	.963	2.03±0.05
124±11			45	6.8±0.2	21.7±0.5	.963	1.89±0.05
124±11			30	6.9±0.2	22.1±0.5	.963	1.92±0.05
141±12			45	6.7±0.2	21.9±0.6	.965	1.91±0.05
141±12	45	7.0±0.2	21.3±0.7	.965	1.86±0.06		
153±13	45	7.2±0.3	19.1±0.7	.966	1.67±0.06		
158±13	45	6.9±0.2	20.4±0.7	.967	1.78±0.06		
169±14	30	7.2±0.3	19.5±0.7	.968	1.70±0.06		
181±15	30	7.2±0.3	18.8±0.6	.969	1.64±0.06		
183±20	T(p, n)	120	7.2±0.3	19.3±0.7	.969	1.69±0.06	
193±15	Li(p, n)	30	7.2±0.3	20.7±0.6	.970	1.80±0.06	
194±20	T(p, n)	75	7.2±0.3	20.0±0.7	.970	1.75±0.06	
217±20	T(p, n)	120	7.2±0.3	18.1±0.6	.972	1.59±0.06	
442±30		75	7.2±0.3	11.6±0.6	.997	1.05±0.06	
648±50		45	7.3±0.4	7.1±0.4	1.015	.65±0.05	
817±70		45	7.3±0.5	5.5±0.4	1.020	.50±0.05	

^aNormalized to 1/v below 80 keV.

TABLE II. - EFFICIENCY OF MODIFIED LONG COUNTER CALIBRATED BY
PRECISION LONG COUNTER FLUX MONITOR

Neutron energy, E_n , keV	Source reaction	Counter angle, deg	Effective center of detection, c, cm	Relative modified long counter count	Efficiency of flux monitor, η_{PLC}	Efficiency of modified long counter, η_{MLC}
39	Li(p, n)	75	5.1±0.1	22.95±0.15	0.953	0.861±0.007
58	↓	75	5.4±0.1	23.45±0.15	.955	.881±0.007
80	↓	75	5.3±0.1	23.50±0.15	.958	.886±0.007
105	↓	45	5.1±0.1	26.00±0.15	.961	.982±0.007
124	↓	45	5.1±0.1	26.20±0.20	.963	.993±0.008
141	↓	45	5.1±0.1	26.00±0.20	.965	.988±0.008
158	↓	45	5.1±0.1	25.95±0.20	.967	.988±0.008
194	T(p, n)	75	5.2±0.1	25.75±0.15	.970	.983±0.007
442	↓	75	5.8±0.1	24.75±0.15	.997	.972±0.007
648	↓	45	6.1±0.1	24.30±0.20	1.015	.971±0.008
817	↓	45	5.8±0.1	23.10±0.15	1.020	.928±0.007
2190	D(d, n)	120	5.9±0.1	17.25±0.15	.980	.665±0.009
3030	↓	75	5.5±0.2	15.95±0.25	.970	.609±0.016
3480	↓	60	5.7±0.2	14.10±0.20	.928	.515±0.015
3900	↓	60	6.5±0.2	12.60±0.20	.916	.454±0.017

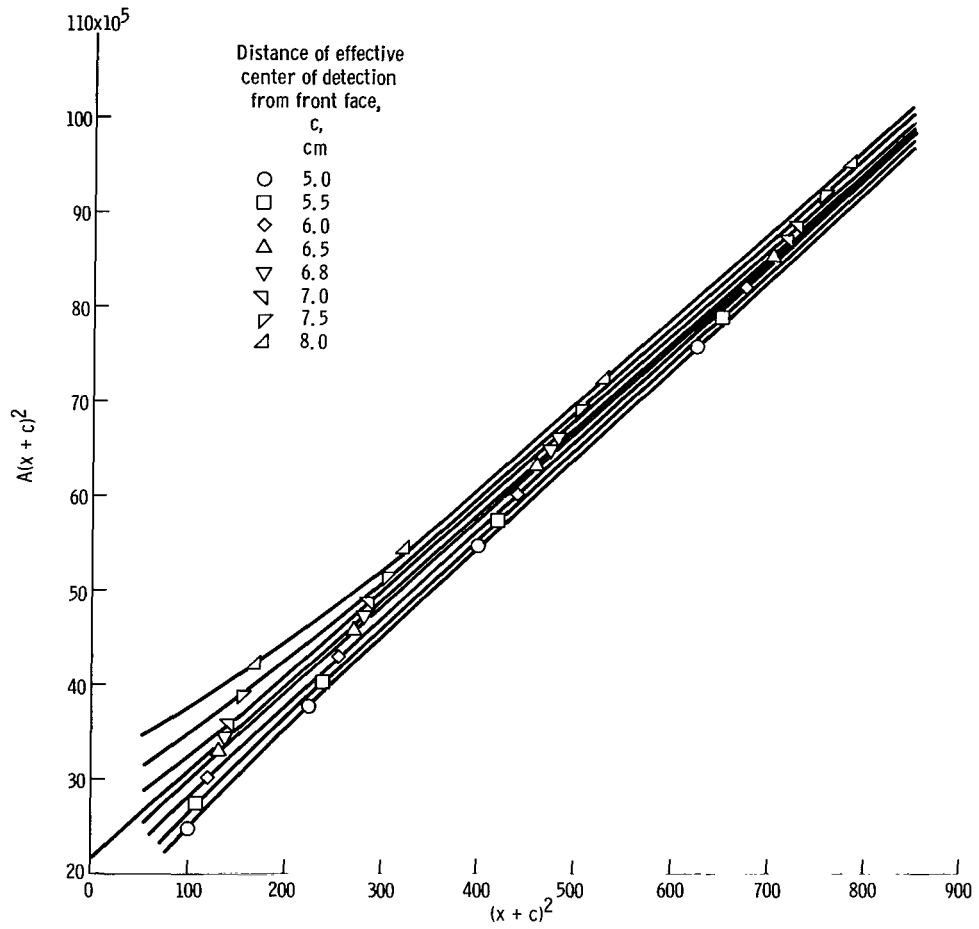


Figure 5. - Analysis of bare BF_3 counter data at detector angle of 45° in various positions from $\text{Li}(p, n)$ source for neutrons of nominal energy of 124 keV. Room-scattered background counts, a, 9080; direct counts, b, $21.7 \pm 0.5 \times 10^5$; distance of effective center of detection from front face, c, 6.8 ± 0.2 centimeters.

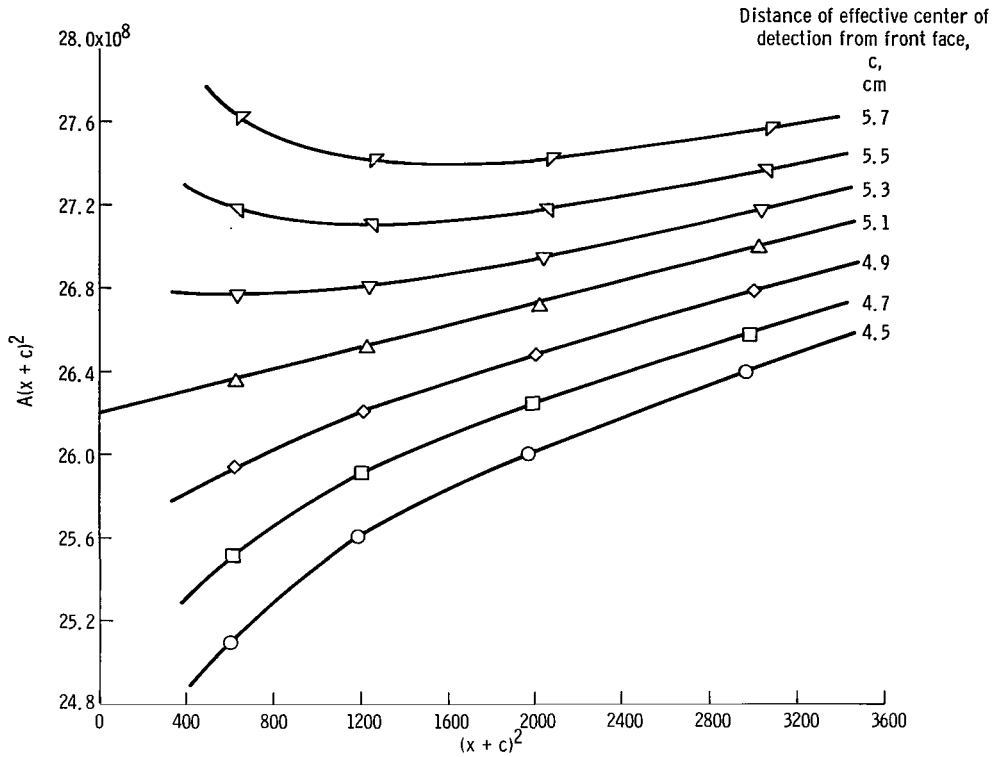


Figure 6. - Analysis of modified long counter data at detector angle of 45° in various positions from $\text{Li}(p, n)$ source for neutrons of nominal energy of 124 keV. Room-scattered background counts, a, $25\,500$; direct counts, b, $26.2 \pm 0.2 \times 10^8$; distance of effective center of detection from front face, c, 5.1 ± 0.1 centimeters.

sides covered with 20 mils (0.508 mm) of cadmium. The background count was reduced by a factor of about 10 with the cadmium in place indicating the bulk of the room-scattered neutrons to be subcadmium. Analysis of both the bare and cadmium covered data in the manner described led to identical values of direct counts with slightly better precision for the cadmium covered data. The large subcadmium component in the background suggests that the assumption of the spatially constant background is a good one.

Table I indicates the best values of c to increase gradually from 6.3 to 7.3 centimeters over the range of energy; these values are to be compared with the distance of the front face of the bare counter to the geometric center of its active volume of 7.7 centimeters. Table II indicates the best values of c , measured from the front face of the paraffin, to increase gradually from 5.1 to 6.5 centimeters; these values are to be compared with the distance to the center of the paraffin of the modified long counter of 6.4 centimeters.

The cross sections $^{10}\text{B}\sigma(n, \alpha)$ of table I are shown in figure 7. A significant deviation from a $1/v$ variation is indicated above 80 keV with departures of 15 percent at 140 keV and 20 percent at 220 keV.

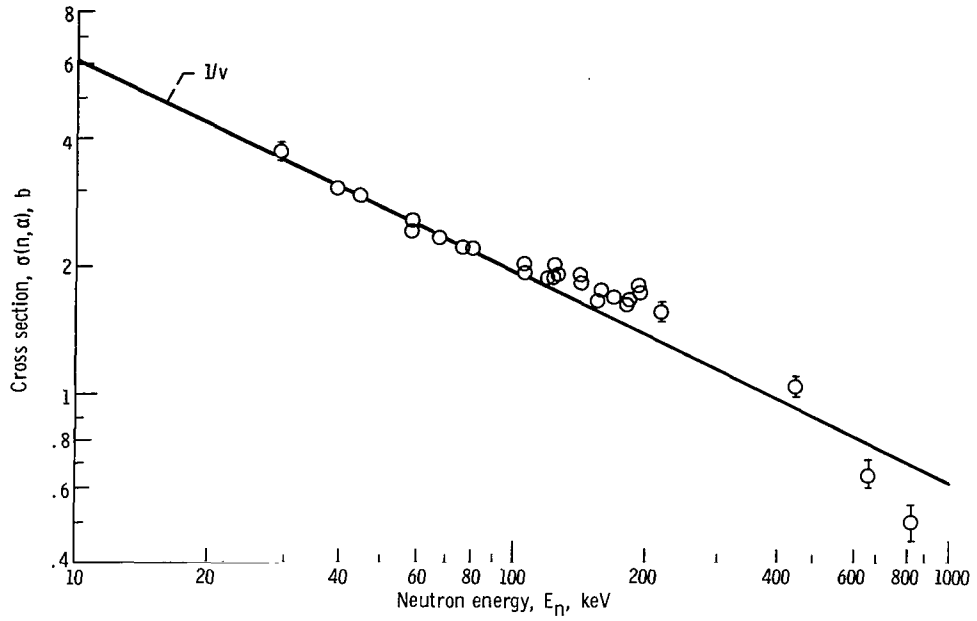


Figure 7. - Present cross sections for $^{10}\text{B}(n, \alpha)^7\text{Li}$, $^7\text{Li}^*$ normalized to $1/v$ variation below 80 keV.

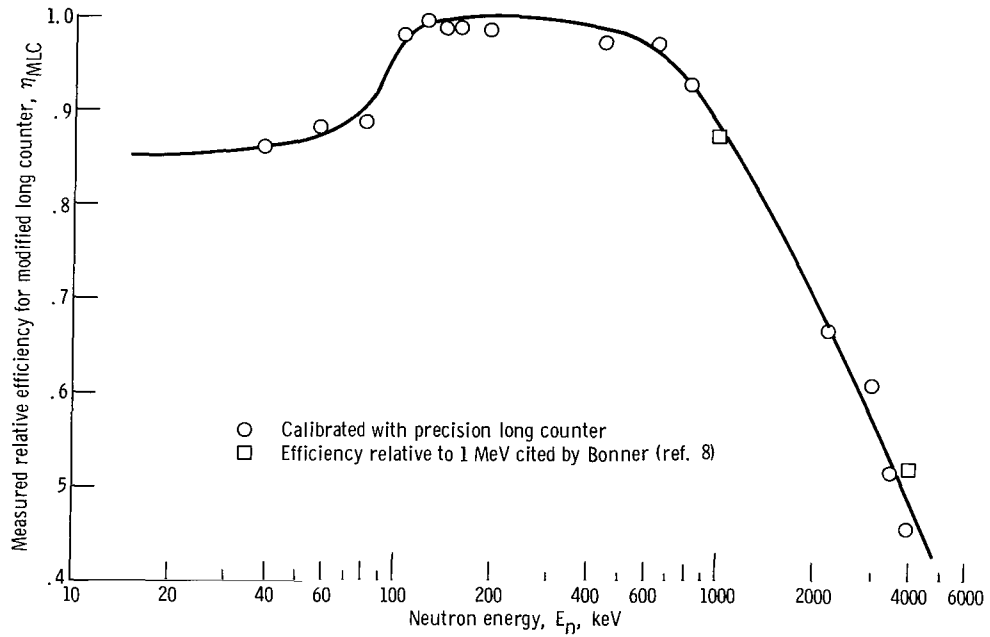


Figure 8. - Measured relative efficiency for modified long counter.

The measured relative efficiency values for the modified long counter η_{MLC} of table II are shown in figure 8. There is a large falloff in efficiency below 100 keV and above 700 keV. The relative efficiency points at 1 and 4 MeV cited by Bonner (ref. 8) are in good agreement with the present results. This efficiency curve is considerably different in shape and in magnitude from the efficiency curve of the same modified long counter estimated by Bogart (ref. 10); therefore, the quantitative variation of $^{10}\text{B}\sigma(n, \alpha)$ suggested in reference 10 overestimated the departures from $1/v$ above 80 keV by 10 to 15 per cent.

Detectors that are similar to the modified long counter are the so-called "Bonner" spheres calibrated by Bramblett, Ewing, and Bonner (ref. 15). These spheres detect neutrons by a small $^6\text{LiI}(\text{Eu})$ scintillator placed at the center of polyethylene moderating spheres with sizes ranging from 5 to 30 centimeters in diameter. Pronounced differences in the efficiencies for the five spheres were observed. One of the spheres was 12.7 centimeters in diameter and, therefore, its neutron response may be compared with that of the modified long counter which is a cylinder 12.7 centimeters in diameter and 12.7 centimeters long. This comparison is made in figure 9 in which remarkably simi-

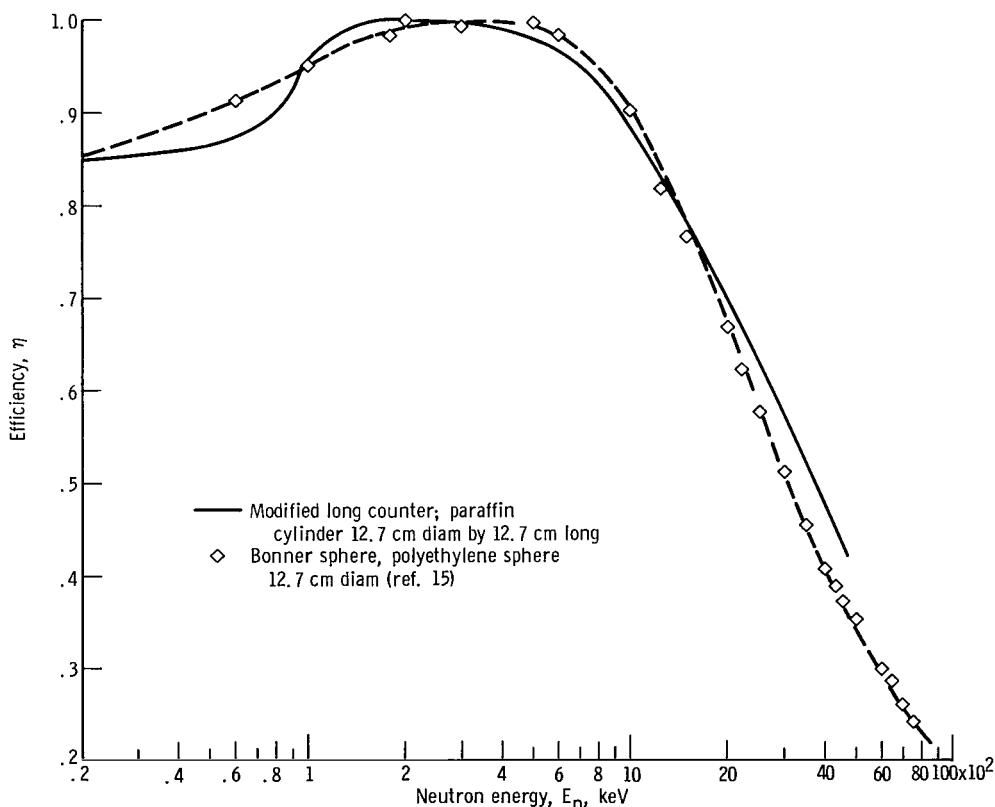


Figure 9. - Comparison of relative efficiency of modified long counter and Bonner sphere.

lar characteristics are observed above 150 keV; below 150 keV, the Bonner sphere suggests a more gradual falloff in efficiency than the modified counter. Therefore, the efficiency curve of the modified counter may be used with an added measure of confidence because of the good agreement.

With the measured efficiency curve of the modified counter, the boron cross sections of Bichsel and Bonner (ref. 7) have been corrected and renormalized to a $1/v$ variation at low energies. The corrected data to 1 MeV are shown in figure 10 and lie above a $1/v$ line in the 80 to 200 keV region with a departure of 15 percent in the 100 to 150 keV region. Above 170 keV, the corrected data fall below the present data. As mentioned before, a source of concern in the experiments of Bichsel and Bonner is the collinear placement of the $^{10}\text{BF}_3$ counter and the modified long counter flux monitor. It is believed that significant $^{10}\text{BF}_3$ counter scattering and modified long counter backscattering effects are present in the data of reference 7 which were not discussed. Therefore, the corrected data curves shown in figure 10 may be subject to shape uncertainties in addition to that due to the use of a flat efficiency curve for the modified long counter.

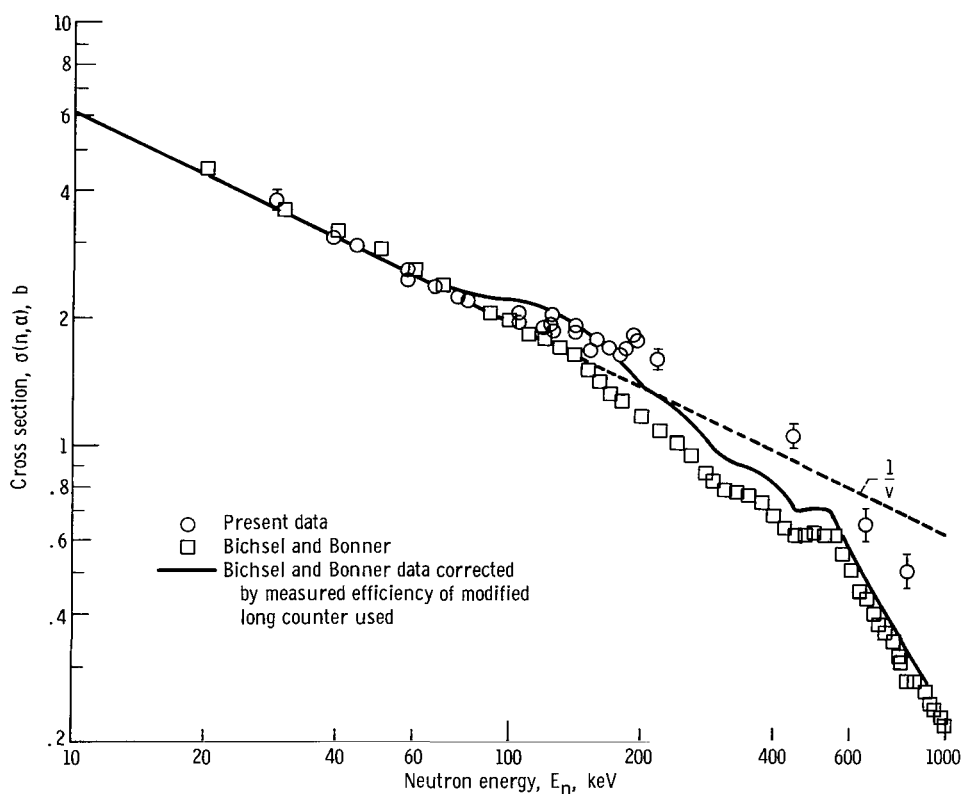


Figure 10. - Cross sections for $^{10}\text{B}(n, \alpha)^7\text{Li}$, $^7\text{Li}^{35}$ corrected for measured efficiency of modified long counter used by Bichsel and Bonner.

DISCUSSION

The available data to 1 MeV for the $^{10}\text{B}(n, \alpha)$ cross section are compared in figure 11. In the lower keV region are shown the present data and that of Macklin and Gibbons (ref. 3) which have been normalized to a $1/v$ variation below 80 keV. The sphere transmission data of Cox (ref. 2) to 250 keV are independent of an absolute flux monitor while the transmission scattering data of Mooring (ref. 1) to 500 keV rely on a symmetrically placed carbon scatterer in a counting system identical to that used for ^{10}B for monitoring the incident neutron flux.

In the higher keV region are shown the data of Davis (ref. 6) and the recent data of Nellis (refs. 4 and 5); these measurements employ conventional long counters to monitor the neutron flux. The long counter used by Davis was constructed according to the recipe of Hanson and McKibben (ref. 9) and absolute neutron flux was obtained comparing counts with a calibrated plutonium-beryllium source placed 1 meter from the long counter. The long counter used by Nellis is a polyethylene long counter of standard size that has been calibrated relative to proton recoil telescopes. The $^{10}\text{B}(n, \alpha_1\gamma)$ cross sections of Nellis have been converted to $^{10}\text{B}(n, \alpha)^7\text{Li}$, $^7\text{Li}^*$ cross sections using the branching ratios of

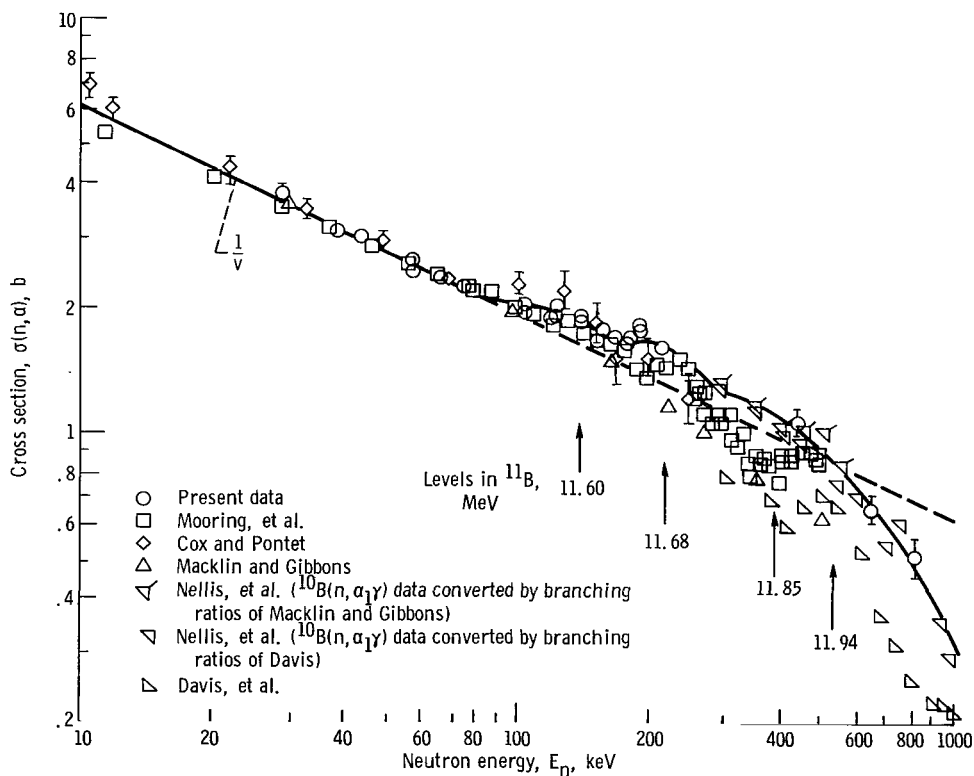


Figure 11. - Comparison of recent measurements and recommended cross sections for $^{10}\text{B}(n, \alpha)^7\text{Li}$, $^7\text{Li}^*$.

Macklin and Gibbons (ref. 3) to 550 keV (tailed symbols) and the branching ratios of Davis (ref. 6) (untailed symbols). These branching ratio measurements differ considerably above 400 keV.

The data of Bichsel and Bonner (ref. 7), which cover the entire range to 1 MeV and have been corrected for the presently measured efficiency of the unconventional modified long counter used, are omitted from figure 11 for clarity, but are shown in figure 10.

It is significant that all data lie above a $1/v$ line to 200 keV. The data of Mooring above 250 keV lie below the $1/v$ line, reverse, and return to $1/v$ at 500 keV. The data of Cox show the largest upside departures from $1/v$ from 100 to 170 keV.

The present data and that of Nellis are in good agreement with our three highest keV points providing a region of overlap. The agreement is good regardless of the spread caused by the different branching ratios used. A recommended cross-section curve has been drawn through these data which lie above the $1/v$ line to 550 keV.

The data of Davis are very much lower than the other data. The quoted uncertainty of these data below 4.5 MeV is ± 20 percent, however, the real error can be larger for energies below 1 MeV. This is based on the results for $^{10}\text{B}(n, t2\alpha)$ cross sections obtained from the pulse-height distributions along with the $^{10}\text{B}(n, \alpha_0)$ and $^{10}\text{B}(n, \alpha_1\gamma)$ results. The $^{10}\text{B}(n, t2\alpha)$ events are seen as a group that is considerably closer to the background counts caused by epithermal (n, α) events but is still reasonably well separated at the higher energies. However, the values of $^{10}\text{B}(n, t2\alpha)$ cross section reported by Davis are compared by him with other published values and found to be considerably lower. This suggests that as pulse-height distributions get closer to epithermal components, separation of groups may be difficult. For neutron energies below 1 MeV, the separation of the $^{10}\text{B}(n, \alpha_1\gamma)$ pulses from epithermal may also be difficult and therefore cross sections for $^{10}\text{B}(n, \alpha_1\gamma)$ may also err in the same manner.

In regard to the data of Macklin and Gibbons which are below the $1/v$ line above 150 keV, it is noted that their method requires accurate branching ratios. This measurement is very difficult as attested to by the large scatter in the various branching-ratio data they compare.

It is clear that several levels are present above 100 keV and that it is necessary to have a large number of data points in this energy range if the contributions of the broad resonance levels are to be discerned. There are at least four energy levels in ^{11}B that can contribute, and these are indicated in figure 11. The 11.60- and 11.85-MeV levels were seen by Bichsel and Bonner in their $^7\text{Li}(\alpha, \alpha)^7\text{Li}^*$ measurements and correspond to a neutron energies of 140 and 390 keV, respectively, in the $^{10}\text{B} + n$ system. The 11.68-MeV level is seen as the broad resonance in their $^7\text{Li}(\alpha, n)^{10}\text{B}$ differential measurements in the forward direction and corresponds to a neutron energy of 220 keV in the $^{10}\text{B} + n$ system. These differential measurements were repeated by Mehta, et al. (ref. 16) who indicate the cross section to rise from threshold and to exhibit a significant

peak in the neighborhood of 4.7 MeV before rising to the prominent peak at 5.15 MeV. Therefore, these differential data suggest resonance structure at alpha energies near 4.7 MeV which corresponds to a level in ^{11}B at 11.68 MeV. The prominent peak at 5.15 MeV corresponds to a channel energy of 530 keV in the $^{10}\text{B} + n$ system. Therefore, the shape of the $^{10}\text{B}(n, \alpha)$ cross sections may be the result of resonances at 140, 220, 390, and 530 keV.

These level locations were considered in estimating the recommended cross section curve represented by the solid line in figure 11. The solid line follows the present data to 220 keV; between 220 and 440 keV the solid line is guided by the data of Nellis; above 440 keV the line represents an average of the present data and that of Nellis. Departures from a $1/v$ variation are noted above 80 keV rising to a 15-percent deviation at 140 keV and to a 20-percent deviation at 220 keV before falling below the $1/v$ line at 550 keV. Above 550 keV, the solid line is about 50 percent higher than the data of Davis, et al.

Lewis Research Center,
National Aeronautics and Space Administration,
Cleveland, Ohio, June 19, 1968,
129-02-04-04-22.

REFERENCES

1. Mooring, F. P.; Monahan, J. E.; and Huddleston, C. M.: Neutron Cross Sections of the Boron Isotopes for Energies Between 10 and 500 keV. Nucl. Phys., vol. 82, 1966, pp. 16-32.
2. Cox, S. A.; and Pontet, F. R.: Measurement of the $^6\text{Li}(n, \text{Absorption})$ and $^{10}\text{B}(n, \text{Absorption})$ Cross Sections by the Shell Transmission Method. J. Nucl. Energy, vol. 21, no. 3, 1967, pp. 271-283.
3. Macklin, R. L.; and Gibbons, J. H.: Study of $^{10}\text{B}(n, \alpha)^7\text{Li}$, $^7\text{Li}^*$ for $30 < E_n < 500$. Phys. Rev., vol. 165, no. 4, Jan. 20, 1968, pp. 1147-1153.
4. Nellis, D. O.; and Morgan, I. L.: Reports to the AEC Nuclear Cross Sections Advisory Group. H. T. Motz, comp. AEC Rep. Wash-1074, EANDC(US)-99U, INDC(US)-9U, Apr. 1967, p. 117.
5. Nellis, D. O.; and Morgan, I. L.: Reports to the AEC Nuclear Cross Sections Advisory Group. M. S. Moore, comp. AEC Rep. WASH-1079, EANDC(US)-104, INDC(US)-12, Oct. 1967, pp. 163-165.
6. Davis, E. A.; Gabbard, F.; Bonner, T. W.; and Bass, R.: The Disintegration of ^{10}B and ^{19}F by Fast Neutrons. Nucl. Phys., vol. 27, 1961, pp. 448-466.

7. Bichsel, Hans; and Bonner, T. W.: Reactions $\text{Li}^7(\alpha, n)\text{B}^{10}$, $\text{Li}^7(\alpha, \alpha')\text{Li}^{7*}$, and $\text{B}^{10}(n, \alpha)\text{Li}^7$. Phys. Rev., vol. 108, no. 4, Nov. 15, 1957, pp. 1025-1027.
8. Bonner, T. W.; Kraus, Alfred A., Jr.; Marion, J. B.; and Schiffer, J. P.: Neutrons and Gamma Rays from the Alpha-Particle Bombardment of ^9Be , ^{10}B , ^{11}B , ^{13}C , and ^{18}O . Phys. Rev., vol. 102, no. 5, June 1, 1956, pp. 1348-1354.
9. Hanson, A. O.; and McKibben, J. L.: A Neutron Detector Having Uniform Sensitivity from 10 Kev to 3 Mev. Phys. Rev., vol. 72, no. 8, Oct. 15, 1947, pp. 673-677.
10. Bogart, Donald: Boron Cross Sections as a Source of Discrepancy for Capture Cross Sections in the keV Region. Neutron Cross Section Technology, P. B. Hemmig, ed. AEC Rep. CONF-660303, Bk. 1, Mar. 24, 1966, pp. 486-501.
11. DePangher, J.: A Reproducible Precision Polyethylene Long Counter for Measuring Fast-Neutron Flux. Bull. Am. Phys. Soc., Ser. II, vol. 6, no. 3, Apr. 24, 1961, p. 252; also Rep. HW-SA-2140, General Electric Co., Apr. 1961.
12. DePangher, J.; and Nichols, L. L.: A Precision Long Counter for Measuring Fast Neutron Flux Density. Rep. BNWL-260, Battelle Northwest, June 1966.
13. Allen, W. H.: Flat Response Counters. Techniques. Part I of Fast Neutron Physics. J. B. Marion and J. L. Fowler, eds., Interscience Publ., 1960, p. 361.
14. DePangher, J.: Double Moderator Neutron Dosimeter. Nucl. Instr. Methods, vol. 5, 1959, pp. 61-74.
15. Bramblett, Richard L.; Ewing, Ronald I.; and Bonner, T. W.: A New Type of Neutron Spectrometer. Nucl. Instr. Methods, vol. 9, 1960, pp. 1-12.
16. Mehta, M. K.; Hunt, W. E.; Plendl, H. S.; and Davis, R. H.: A Study of the $^6\text{Li}(\alpha, n)^9\text{B}$ and $^7\text{Li}(\alpha, n)^{10}\text{B}$ Reactions. Nucl. Phys., vol. 48, 1963, pp. 90-96.

FIRST CLASS MAIL

POSTMASTER: If Undeliverable (Section 158
Postal Manual) Do Not Return

"The aeronautical and space activities of the United States shall be conducted so as to contribute . . . to the expansion of human knowledge of phenomena in the atmosphere and space. The Administration shall provide for the widest practicable and appropriate dissemination of information concerning its activities and the results thereof."

— NATIONAL AERONAUTICS AND SPACE ACT OF 1958

NASA SCIENTIFIC AND TECHNICAL PUBLICATIONS

TECHNICAL REPORTS: Scientific and technical information considered important, complete, and a lasting contribution to existing knowledge.

TECHNICAL NOTES: Information less broad in scope but nevertheless of importance as a contribution to existing knowledge.

TECHNICAL MEMORANDUMS: Information receiving limited distribution because of preliminary data, security classification, or other reasons.

CONTRACTOR REPORTS: Scientific and technical information generated under a NASA contract or grant and considered an important contribution to existing knowledge.

TECHNICAL TRANSLATIONS: Information published in a foreign language considered to merit NASA distribution in English.

SPECIAL PUBLICATIONS: Information derived from or of value to NASA activities. Publications include conference proceedings, monographs, data compilations, handbooks, sourcebooks, and special bibliographies.

TECHNOLOGY UTILIZATION PUBLICATIONS: Information on technology used by NASA that may be of particular interest in commercial and other non-aerospace applications. Publications include Tech Briefs, Technology Utilization Reports and Notes, and Technology Surveys.

Details on the availability of these publications may be obtained from:

**SCIENTIFIC AND TECHNICAL INFORMATION DIVISION
NATIONAL AERONAUTICS AND SPACE ADMINISTRATION
Washington, D.C. 20546**